Theoretical investigation of magnetic order in *R*FeAsO (*R*=Ce,Pr)

H. M. Alyahyaei and R. A. Jishi
Department of Physics, California State University, Los Angeles, California 90032, USA
(Received 15 November 2008; revised manuscript received 15 January 2009; published 17 February 2009)

Density-functional theory calculations are carried out on *R*FeAsO, *R*=Ce and Pr, the parent compounds of the high-T_c superconductors $R\mathrm{FeAsO}_{1-x}\mathrm{F}_x$, in order to determine the magnetic order of the ground state. It is found that the magnetic moments on the Fe sites adopt an antiferromagnetic order, with a stripelike pattern similar to the case of LaFeAsO. Within the generalized gradient approximation along with Coulomb on-site repulsion (GGA+U), we show that the *R* magnetic moments also adopt an antiferromagnetic order for which, within the *R*O layer, the same spin *R* sites lie along a zigzag line perpendicular to the Fe spin stripes. While within GGA the *R* 4*f* band crosses the Fermi level, upon inclusion of on-site Coulomb interaction on the *R* sites the 4*f* band splits and moves away from the Fermi level. If on-site Coulomb interaction is also included on the Fe sites, *R*FeAsO is shown to change from a semimetal to a Mott insulator.

DOI: 10.1103/PhysRevB.79.064516 PACS number(s): 74.25.Ha, 74.25.Jb

I. INTRODUCTION

Recently, a new class of layered iron-based high-temperature superconductors has been discovered. Kamihara *et al.*[1] reported a superconducting transition temperature T_c =26 K in fluorine-doped LaFeAsO. This is a member of a family of compounds known as quaternary oxypnictides with a general formula Ln*M*PnO, where Ln is a lanthanide (La, Ce, Pr, etc.), M is a transition metal (Mn, Fe, Co, etc.), and Pn is a pnicogen (P, As, etc.). Shortly afterward, it was shown[2] that under pressure the transition temperature increased to 43 K. Replacement of La with other rare-earth elements gave a series of superconducting compounds $R\mathrm{FeAsO}_{1-x}\mathrm{F}_x$ with *R*=Ce, Pr, Nd, Sm, or Gd, with transition temperatures close to or exceeding 50 K.[3–9] Hole doping, achieved by replacing La with Sr or Gd with Th, was also found to yield superconducting compounds.[10,11] Oxygen-deficient samples were also synthesized and found to superconduct at 55 K.[12–14] Using high-pressure techniques, it was possible to increase the concentration of the F-dopant[15] and to synthesize superconducting compounds where La is replaced by the late rare-earth elements Tb and Dy.[16,17]

The parent compound, *R*FeAsO, is a layered compound consisting of a stack of alternating *R*O and FeAs layers. At high temperatures, the crystal structure is tetragonal with space group $P4/nmm$ and a unit cell, shown in Fig. 1, which contains two molecules. But at low temperatures, the crystal undergoes a structural phase transition to an orthorhombic phase with *Cmma* space group and a unit cell that contains four molecules.[18–22]

The FeAs layer consists of a square planar sheet of Fe sandwiched between two sheets of As. Similarly, the *R*O layer consists of an oxygen sheet sandwiched between two *R* sheets. Upon fluorine doping these compounds become superconductors. It is not understood at this stage what mechanism lies behind superconductivity in these compounds. Understanding the electronic structure of the undoped parent compounds is necessary to understand the doped compounds, especially that in these iron-based compounds, there is an interplay between magnetism and superconductivity, as is the case in the high-T_c cuprates.

Initial calculations using density-functional theory (DFT) concluded that LaFeAsO is metallic and nonmagnetic (NM) but with possible antiferromagnetic (AFM) fluctuations.[23–25] More extensive calculations on states with various possible magnetic orders in LaFeAsO, however, showed that the magnetic moments of the Fe ions are ordered antiferromagnetically in a stripelike pattern in the Fe plane, resulting in a magnetic unit cell with $\sqrt{2}a\times\sqrt{2}a\times c$ supercell structure, in contrast to the nuclear axaxc unit cell.[26–31] Indeed, neutron-scattering measurements on undoped parent compounds reveal the existence of such an AFM state at low temperatures.[18–22] Upon doping, the magnetic order is suppressed, and as the temperature is lowered the superconducting state emerges. This leads to the reasonable belief that strong electronic correlations are important in these systems and that superconductivity in these compounds is somehow connected to magnetic fluctuations.[25–37]

In this work we study the electronic structure of the parent compounds *R*FeAsO, *R*=Ce and Pr, using DFT within the generalized gradient approximation (GGA). We consider

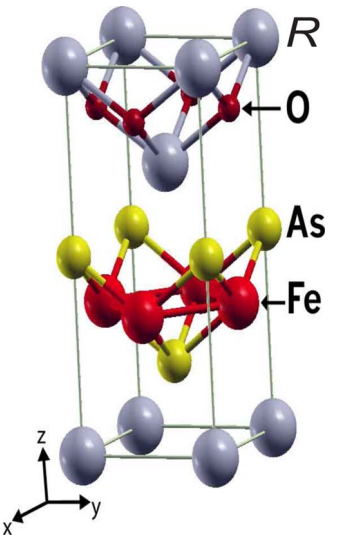

FIG. 1. (Color online) The high-temperature teteragonal unit cell of *R*FeAsO, where *R* stands for a rare-earth atom.

various possible magnetic orders of the Fe and R ions. We show that in the ground state the magnetic moments of the Fe ions adopt an AFM order with a stripelike pattern, as in the case of LaFeAsO. Within GGA the Ce sites are paramagnetic (PM), but when the on-site Coulomb interaction is taken into account (GGA+U), the magnetic moments on the Ce sites, resulting from the 4f electrons, also adopt an AFM order with a zigzaglike pattern. On the other hand, within both GGA and GGA+U, the magnetic moments on the Pr sites adopt an AFM order similar to that on the Ce sites.

II. METHOD

The first-principles calculations presented in this work were performed using the all-electron full potential linear augmented plane wave plus local orbitals (FP-LAPW+lo) method as implemented in WIEN2K code.[38] In this method the core states are treated in a fully relativistic way, but the valence states are treated at a scalar relativistic level. The exchange-correlation potential was calculated using the GGA as proposed by Pedrew *et al.*[39]

For calculations in this work, the crystal is taken to be orthorhombic, being the low temperature phase, with space group *Cmma*. The lattice constants are $a=5.662\,63$ Å, $b=5.632\,73$ Å, and $c=8.6444$ Å, in the case of CeFeAsO,[19] and $a=5.6374$ Å, $b=5.6063$ Å, and $c=8.5966$ Å, in the case of PrFeAsO.[20] In the low-temperature orthorhombic phase, the unit cell has four R atoms with crystal coordinates $R1(0,0.25,z)$, $R2(0,0.75,-z)$, $R3(0.5,0.25,-z)$, and $R4(0.5,0.75,z)$, where $z=0.1402$ or 0.1385 for R=Ce or Pr, respectively. $R1$ and $R4$ belong to an R plane above the O plane, while $R2$ and $R3$ belong to an R plane below the O plane. These two R planes, along with the O plane sandwiched between them, constitute the RO layer. The radii of the muffin-tin spheres are chosen so that the nearby muffin-tin spheres are almost touching. For all structures considered in this work we set the parameter $R_{\mathrm{MT}}K_{\mathrm{max}}=7$, where R_{MT} is the smallest muffin-tin radius and K_{max} is a cutoff wave vector. The valence wave functions inside the muffin-tin spheres are expanded in terms of spherical harmonics up to $l_{\mathrm{max}}=10$, while in the interstitial region they are expanded in plane waves with a wave vector cutoff K_{max}, and the charge density is Fourier expanded up to $G_{\mathrm{max}}=13a_0^{-1}$, where a_0 is the Bohr radius. Convergence of the self-consistent field calculations is attained with a strict charge convergence tolerance of 0.000 01e.

III. RESULTS AND DISCUSSION

To begin with, we consider within GGA various magnetic orders of the Fe magnetic moments in the Fe plane: nonmagnetic, ferromagnetic (FM), checkerboard antiferromagnetic (c-AFM), and antiferromagnetic with stripelike pattern (s-AFM). We find that the s-AFM order of the Fe magnetic moments has the lowest energy. The energy of the s-AFM order of the Fe moments is lower than the c-AFM order by 0.031 eV/Fe atom, lower than the FM order by 0.156 eV/Fe atom, and lower than the nonmagnetic phase by 0.146 eV/Fe atom. In the c-AFM order, every spin-up Fe site is surrounded by four nearest-neighbor (NN) spin-down Fe sites, whereas in the s-AFM order, among the four NN Fe sites surrounding a spin-up Fe site, two along the b-axis are spin up and the other two along the a-axis are spin down, but the four next-nearest-neighbor (NNN) Fe sites are all spin down. The c-AFM and the s-AFM orders within the Fe plane were described elsewhere[18,26–29] in connection with LaFeAsO. That the ground state has s-AFM order of the Fe magnetic moments, in CeFeAsO and PrFeAsO, is consistent with what has already been found in LaFeAsO (Refs. 18 and 26–29) and with neutron-diffraction measurement on these crystals.[19,20] The s-AFM order in the FeAs layer is shown in Fig. 2(a).

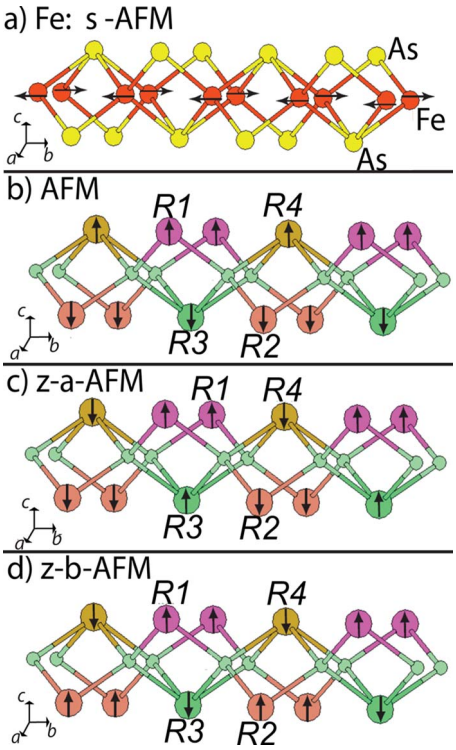

FIG. 2. (Color online) The various antiferromagnetic orders in RFeAsO. In (a), a single FeAs layer is shown with Fe spin stripes along the b direction. In (b)–(d), a single RO layer is shown; it is composed of one oxygen plane sandwiched between two R planes. In (b), the AFM order shown is such that each spin-up R site, on a given plane, has four nearest-neighbor spin-down R sites on the other R plane of the layer. In (c), the z-a-AFM order is shown. Here, if nearest-neighboring spin-up R sites are connected, the result is a zigzag chain running along the a axis; the same holds if nearest-neighboring spin-down R sites are connected. In (d), the z-b-AFM magnetic order is shown; it is similar to z-a-AFM except that now the same-spin zigzag chains connecting nearest neighboring R sites run along the b direction.

In the remaining calculations we fix the spin order within the Fe plane to be s-AFM, with the Fe spin stripes taken to be along the b direction in the magnetic unit cell. A spin-up stripe in the a-b plane is a line of Fe ions, parallel to the b axis, with up spins; this is surrounded in the a-b plane by two spin-down stripes, also parallel to the b axis. Fixing the spin order in the Fe plane, we now focus our attention on the spin order of the R ions. Considering only the R sites in

*R*FeAsO, we note that every *R* site (for example, Ce1) has four NN *R* sites (two Ce2 sites at a distance of 3.72 Å and two Ce3 sites at a distance of 3.73 Å) and four NNN *R* sites (four Ce4 sites at a distance of 3.998 Å). Thus for the magnetic order on the *R* sites we consider six different cases.

(1) The NM phase, where the magnetic moment on every *R* site is constrained to be zero.

(2) The PM phase, where the magnetic moment on each *R* site is nonzero, but the spins on different *R* sites are not correlated.

(3) The FM order, where the magnetic moments on all *R* sites are aligned in the same direction.

(4) The AFM order, where the four *R* ions in the unit cell, *R*1-*R*2-*R*3-*R*4, whose crystal coordinates were given earlier, have the spin arrangement uddu, where *u* stands for up and *d* stands for down. In this phase, considering an *R*O layer (one O plane surrounded by two *R* planes) the *R* spins in one plane are all up, while the *R* spins in the other plane are all down. That is, in each *R* plane the order is FM, but the magnetization in one *R* plane is opposite to that in the nearby *R* plane lying across from the O plane. The AFM order in the *R*O layer is depicted in Fig. 2(b).

(5) The zigzag-along-a antiferromagnetic (z-a-AFM) order where a spin-up *R* site has two NN spin-down *R* sites, two NN spin-up *R* sites, and four NNN spin-down *R* sites. The four *R* ions in the unit cell, *R*1-*R*2-*R*3-*R*4, have the spin arrangement udud, as shown in Fig. 2(c). Here, if we connect the same-spin NN *R* ions in a given *R*O layer, we obtain a zigzag chain running parallel to the *a*-axis direction. In this phase, if we consider a single *R* plane (for example, the one containing *R*1 and *R*4), then it is clear that the *R* magnetic moments in this plane adopt a simple AFM order where each spin up *R* ion (for example, *R*1) is surrounded by four spin-down *R* ions (four *R*4 ions). So in each of the two *R* planes surrounding the O-plane in the *R*O layer, the magnetic order is AFM in such a way as to produce same-spin zigzag chains running along the *a* direction.

(6) The zigzag-along-b antiferromagnetic (z-b-AFM) order for which the four *R* ions in the unit magnetic cell, *R*1-*R*2-*R*3-*R*4, have the spin arrangement uudd; this magnetic order is shown in Fig. 2(d). This is similar to case 5 except that the same-spin *R* ions lie on zigzag chains running along the *b* direction. In an isolated *R*O layer, and assuming that *R*1-*R*2 separation is the same as *R*1-*R*3 separation, this phase will have the same energy as the previous z-a-AFM phase. But because in the orthorhombic structure *R*1-*R*2 separation is slightly less than *R*1-*R*3 separation, and the Fe plane has spin stripes along the *b* axis, it follows that these two phases will not be degenerate, particularly if the Fe and *R* spins interact.

We should note that the three antiferromagnetic orders considered above constitute the possible AFM orders of the *R* magnetic moments within the assumed unit cell. It is always possible to consider a larger unit cell and allow for many more possible magnetic orders. The calculations, however, will be far more complicated, and a strong justification for carrying out such a program is lacking. Neutron-diffraction measurements[18–22] are consistent with the orthorhombic unit cell used in our calculations.

We make the following two remarks about how the calculations are performed.

(i) It is not really possible to calculate directly the total energy of the PM phase because in this phase the magnetic moments on the *R* sites are randomly oriented; it follows that a unit cell in the PM phase will contain a very large number of *R* atoms. On the other hand, the average magnetic moment per *R* site is zero in the PM phase. Therefore, one way to calculate the total energy of the PM phase is to constrain the magnetic moment on every *R* site to be zero; this will make the total energy of the PM phase coincide with that of the NM phase, which is not the case in reality. To get around this problem we note that in the high temperature γ phase of elemental cerium crystal, the NN distance between Ce atoms is 3.65 Å (Ref. 40) and that in this phase, while the 6*s* and 5*d* valence electrons are itinerant, the $4f^1$ electron is localized on the Ce site, giving rise to a localized magnetic moment. In CeFeAsO the distance between the NN Ce sites is 3.72 Å, slightly larger than in γ-phase Ce; hence we expect that here the 4*f* electrons are strongly localized on the Ce sites, giving rise to magnetic moments localized on these sites. We calculate the total energy of an isolated Ce atom for both cases when the atom is nonmagnetic (half the $4f^1$ electron is spin up, and the other half is spin down) and when it is magnetic. We find that the energy difference is

$$E_{\text{magnetic}}(\text{Ce}) - E_{\text{nonmagnetic}}(\text{Ce}) = -0.168 \text{ eV}.$$

Therefore, we make the reasonable assumption that 0.168 eV/Ce ion approximates the energy difference between the energies of CeFeAsO in the PM phase (Fe ions have s-AFM order but Ce ions are paramagnetic) and in the NM phase (Fe ions have s-AFM order while Ce ions are nonmagnetic). Similarly, the energy of the magnetic Pr atom is found to be lower than that of the nonmagnetic one by 0.193 eV. We note that whether we follow this scheme or treat a paramagnetic *R* ion as simply nonmagnetic, our final conclusion with regard to the magnetic order in the ground state of *R*FeAsO will be the same.

(ii) In doing the GGA+*U* calculations, we need the value of *U*-*J*, where *U* is the on-site Coulomb repulsion and *J* is the exchange coupling. For Fe, $J \simeq 0.9$ eV, and *U* has an empirical value in the range of 3.5–5.1 eV (Ref. 41); in our calculation we take $U\text{-}J = 3.4$ eV for the Fe ions. For the Ce ions, values for *U*-*J* ranging from 2 to 5 eV for GGA calculations are found in the literature,[42–44] though the value $U\text{-}J = 5$ eV appears to give better results in describing the electronic structure of cerium oxides. For Pr values as large as 6 eV, were reported for *U*-*J* in some oxide of Pr.[45] In the calculations reported here we consider two cases where *U*-*J* is taken to be 3 or 5 eV for both Ce and Pr.

A summary of the total-energy calculations is given in Table I, where we report the differences in the total energy among the six cases listed earlier. We take the energy of the NM phase, in which the Fe moments adopt s-AFM order and the Ce ions are nonmagnetic, as our zero energy. The results in Table I show that within GGA, in the absence of the on-site Coulomb interaction, the ground state of CeFeAsO is one where the Fe magnetic moments adopt s-AFM order while the Ce sites are paramagnetic. In the presence of the on-site Coulomb interaction, on the other hand, the Fe magnetic moments adopt the s-AFM order and the Ce magnetic

TABLE I. The relative energies per R ion in five different magnetic orders of the R ions in RFeAsO. In all these phases, the PM, FM, AFM, z-a-AFM, and z-b-AFM, the magnetic order refers only to the magnetic moments on the R sites. In all these phases, the magnetic moments of the Fe ions are ordered in a s-AFM with Fe spin stripes in the Fe plane taken to be parallel to the b axis. The zero of energy corresponds to the case where the R ion is nonmagnetic. Here $U'=U$-J, where U is the on-site Coulomb interaction and J is the exchange coupling.

	Energy (eV/R)				
Phase	PM	FM	AFM	z-b-AFM	z-a-AFM
		R=Ce			
GGA	−0.168	0.0056	−0.0127	−0.0054	−0.006 23
GGA+U, U'=3 eV	−0.168	−0.489	−0.528	−0.538	−0.583
GGA+U, U'=5.0 eV	−0.168	−0.452	−0.490	−0.494	−0.551
		R=Pr			
GGA	−0.193	−0.466	−0.461	−0.460	−0.473
GGA+U, U'=3 eV	−0.193	−0.504	−0.534	−0.523	−0.534
GGA+U, U'=5.0 eV	−0.193	−0.531	−0.550	−0.532	−0.552

moments the z-a-AFM order. For the case of PrFeAsO, our results indicate that the Pr magnetic moments also adopt the z-a-AFM order both within GGA and GGA+U. Indeed, the antiferromagnetic ordering of the magnetic moments on the Ce sites has been inferred from low-temperature specific heat measurements.[4] Furthermore, neutron-diffraction measurements also revealed an antiferromagnetic order, at low temperatures, of the R magnetic moments in RFeAsO for R=Ce, Pr, and Nd.[19–21]

Next, we turn to the calculation of the electronic density of states (DOS) in the ground-state configuration determined

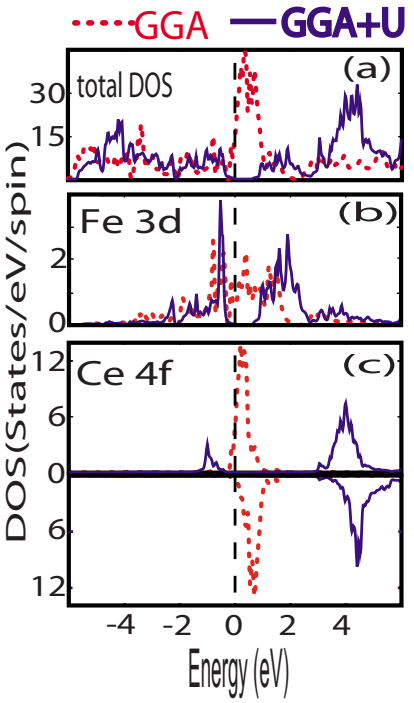

FIG. 3. (Color online) Spin-resolved DOS in CeFeAsO in the {Fe: s-AFM; Ce: z-a-AFM} phase within GGA (red) and GGA+U (blue). The zero energy is the Fermi energy. In (a) the total DOS is shown, while (b) and (c) show the orbital-resolved atomic DOS due to Fe 3d and Ce 4f states, respectively. In (c) the upper panel displays the spin-up DOS, while the lower one displays the spin-down DOS. Note that within GGA+U, a gap opens up at the Fermi energy.

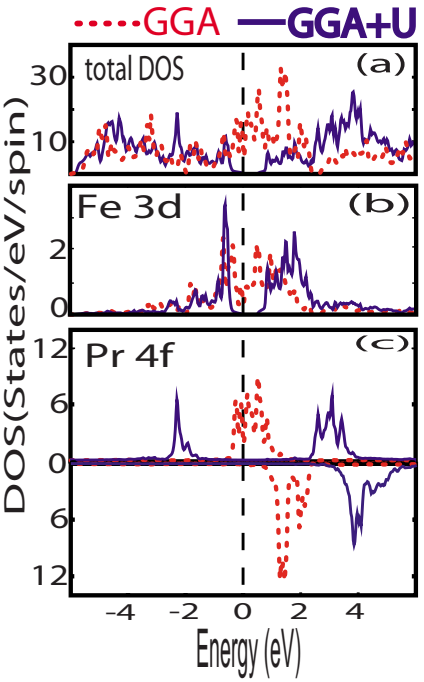

FIG. 4. (Color online) Spin-resolved DOS in PrFeAsO in the {Fe: s-AFM; Pr: z-a-AFM} phase within GGA (red) and GGA+U (blue). The zero energy is the Fermi energy. In (a) the total DOS is shown, while (b) and (c) show the orbital-resolved atomic DOS due to the Fe 3d and Pr 4f states, respectively. In (c) the upper panel displays the spin-up DOS, while the lower one displays the spin-down DOS. Within GGA+U, a gap opens up at the Fermi level.

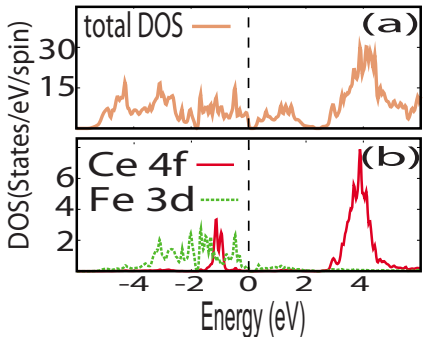

FIG. 5. (Color online) DOS in CeFeAsO for the case with on-site Coulomb repulsion only on the Ce sites. The zero energy is the Fermi energy. The upper panel shows the total DOS; the DOS is nonzero at the Fermi energy, indicating the semimetallic nature of this compound. In the lower panel, the atomic densities of states due to the 3*d* states on one Fe atom and the 4*f* states on one Ce atom are shown. The Fe 3*d* DOS is nonvanishing at the Fermi level.

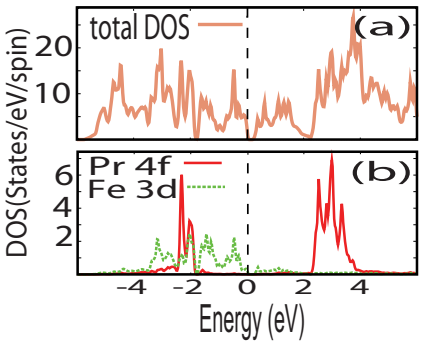

FIG. 6. (Color online) DOS in PrFeAsO for the case with on-site Coulomb repulsion only on the Pr sites. The zero energy is the Fermi energy. The upper panel shows the total DOS; the DOS is nonzero at the Fermi energy, indicating the semimetallic nature of this compound. In the lower panel, the atomic densities of states due to the 3*d* states on one Fe atom and the 4*f* states on one Pr atom are shown. The Fe 3*d* DOS is nonvanishing at the Fermi level.

above. Nekrasov *et al.*[46] carried out calculations, within the local-density approximation, whereby the 4*f* shells of *R* were treated as core states; their results indicated that the electronic energy bands were insensitive to the variation of *R* from La to Sm. Similar band calculations were also reported by Pourovskii *et al.*[47] where the on-site Coulomb repulsion on the *R* sites was taken into account, the 4*f* states now being treated as valence states. Their calculated DOS show the presence of two narrow peaks, associated with the 4*f* bands, one below and one above the Fermi level.

Our calculated electronic DOSs in *R*FeAsO in the phase {Fe: s-AFM; *R*: z-a-AFM} are shown in Figs. 3 and 4, as calculated within GGA and GGA+*U*, for *R*=Ce and Pr. In Fig. 3 we display the total DOS and the Fe 3*d* and Ce 4*f* partial DOS in CeFeAsO for both GGA and GGA+*U*; in the GGA+*U* calculation we consider the on-site Coulomb interaction on both Fe and Ce. The corresponding results in PrFeAsO are shown in Fig. 4. For both compounds, the GGA calculation produces an Fe 3*d* band and a narrow *R* 4*f* band both crossing the Fermi level. The DOS at the Fermi energy is dominated by 4*f* states, making *R*FeAsO, within GGA, a metal. With on-site Coulomb interaction taken into account, *R*FeAsO becomes a Mott insulator. By examining the DOS plots, it is noted that within GGA+*U*, the *R* 4*f* band splits and moves away from the Fermi level.

In Fig. 5, we display the DOS in CeFeAsO for the case when the on-site Coulomb repulsion is taken into account only on the Ce sites but not on Fe sites. In this case, the compound is found to be a semimetal, with a small but finite DOS at the Fermi energy resulting from the Fe 3*d* states. The corresponding results for PrFeAsO are shown in Fig. 6. Our results in Figs. 5 and 6 are generally in good agreement with the calculations by Pourovskii *et al.*[47] In their calculations the split *R* 4*f* bands move further away from the Fermi energy than in our calculations; this is due to the much larger value for *U*-*J* used in their calculations than in ours. Excluding the *R* 4*f* bands, our results show that the electronic structure of the CeFeAsO and PrFeAsO compounds are similar to LaFeAsO: within GGA LaFeAsO is semimetallic[26–31] but with on-site Coulomb repulsion on the Fe sites taken into account, it turns into a Mott insulator with a small energy gap.[25]

IV. CONCLUSIONS

In conclusion, the DFT calculations indicate that the Fe magnetic moments in *R*FeAsO, *R*=Ce and Pr, adopt an antiferromagnetic order with a stripelike pattern similar to that in LaFeAsO. Whereas the La ion in LaFeAsO is nonmagnetic, the *R* ion in *R*FeAsO carries a magnetic moment due to its localized 4*f* electrons. Within GGA+*U*, we show that the *R* magnetic moments also adopt an antiferromagnetic order similar to that adopted by the Fe ions. However, while the Fe ions in the FeAs layer all lie in one plane, giving rise to an AFM order with a stripelike pattern, the *R* ions in the *R*O layer lie in two different planes surrounding the oxygen ions plane. In each *R* plane, an *R* ion is surrounded by four *R* ions that have spins opposite to the spin of the central ion. Viewed in this light, we can say that in the ground state within each *R* plane, the spin order is simply antiferromagnetic, where each spin-up site is surrounded by four spin-down sites in the same plane. However, for a given spin-up *R* ion in a given *R* plane, its four NN *R* ions all lie in the other *R* plane of the *R*O layer; of those four NN *R* ions, two will be spin up and two will be spin down. If we connect each spin-up *R* site to its NN spin-up sites within a given *R*O layer, we will end up with a zigzag chain running perpendicular to the Fe spin stripes in the Fe plane. A similar zigzag chain is obtained if we connect NN spin-down *R* sites within any one *R*O layer.

[1] Y. Kamihara, T. Watanabe, M. Hirano, and H. Hosono, J. Am. Chem. Soc. **130**, 3296 (2008).
[2] H. Takahashi, K. Igawa, K. Arii, Y. Kamihara, M. Hirano, and H. Hosono, Nature (London) **453**, 376 (2008).
[3] D. A. Zocco, J. J. Hamlin, R. E. Baumbach, M. B. Maple, M. A. McGuire, A. S. Sefat, B. C. Sales, R. Jin, D. Mandrus, J. R. Jeffries, S. T. Weir, and Y. K. Vohra, Physica C **468**, 2229 (2008).
[4] G. F. Chen, Z. Li, D. Wu, G. Li, W. Z. Hu, J. Dong, P. Zheng, J. L. Luo, and N. L. Wang, Phys. Rev. Lett. **100**, 247002 (2008).
[5] Z. Ren, J. Yang, W. Lu, W. Yi, G. Che, X. Dong, L. Sun, and Z. Zhao, Mater. Res. Innovations **12**, 105 (2008).
[6] Z. A. Ren, J. Yang, W. Lu, W. Yi, X. Shen, Z. Li, G. Che, X. Dong, L. Sun, F. Zhou, and Z. Zhao, Europhys. Lett. **82**, 57002 (2008).
[7] X. H. Chen, T. Wu, G. Wu, R. H. Liu, H. Chen, and D. F. Fang, Nature (London) **453**, 761 (2008).
[8] Z. A. Ren, W. Lu, J. Yang, W. Yi, X. L. Shen, Z. Li, G. Che, X. Dong, L. Sun, F. Zhou, and Z. Zhao, Chin. Phys. Lett. **25**, 2215 (2008).
[9] P. Cheng, L. Fang, H. X. Yang, X. Zhu, G. Mu, H. Luo, Z. Wang, and H. Wen, Sci. China, Ser. G **51**, 719 (2008).
[10] H. H. Wen, G. Mu, L. Fang, H. Yang, and X. Y. Zhu, Europhys. Lett. **82**, 17009 (2008).
[11] C. Wang, L. Li, S. Chi, Z. Zhu, Z. Ren, Y. Li, Y. Wang, X. Lin, Y. Luo, S. Jiang, X. Xu, G. Cao, and Z. Xu, Europhys. Lett. **83**, 67006 (2008).
[12] J. Yang, Z. Li, W. Lu, W. Yi, X. Shen, Z. Ren, G. Che, X. Dong, L. Sun, F. Zhou, and Z. Zhao, Supercond. Sci. Technol. **21**, 082001 (2008).
[13] G. Wu, H. Chen, Y. L. Xie, Y. J. Yan, T. Wu, R. H. Liu, X. F. Wang, D. F. Fang, J. J. Ying, and X. H. Chen, Phys. Rev. B **78**, 092503 (2008).
[14] Z.-A. Ren, G. C. Che, X.-L. Dong, J. Yang, W. Lu, W. Yi, X. L. Shen, Z. Li, L. Sun, F. Zhou, and Z. Zhao, Europhys. Lett. **83**, 17002 (2008).
[15] W. Lu, X.-L. Shen, J. Yang, Z.-C. Li, W. Yi, Z.-A. Ren, X.-L. Dong, G.-C. Che, L.-L. Sun, F. Zhou, and Z.-X. Zhao, Solid State Commun. **148**, 168 (2008).
[16] J.-W. G. Bos, G. B. S. Penny, J. A. Rodgers, D. A. Sokolov, A. D. Huxley, and J. P. Attfield, Chem. Commun. (Cambridge) **2008**, 3634.
[17] L. J. Li, Y. K. Li, Z. Ren, Y. K. Luo, X. Lin, M. He, Q. Tao, Z. W. Zhu, G. H. Cao, and Z. A. Xu, Phys. Rev. B **78**, 132506 (2008).
[18] C. de la Cruz, Q. Huang, J. W. Lynn, J. Y. Li, W. Ratcliff, J. L. Zarestky, H. A. Mook, G. F. Chen, J. L. Luo, N. L. Wang, and P. C. Dai, Nature (London) **453**, 899 (2008).
[19] J. Zhao, Q. Huang, C. de la Cruz, S. Li, J. W. Lynn, Y. Chen, M. A. Green, G. F. Chen, G. Li, Z. Li, J. L. Luo, N. L. Wang, and P. Dai, Nature Mater. **7**, 953 (2008).
[20] J. Zhao, Q. Huang, C. de la Cruz, J. W. Lynn, M. D. Lumsden, Z. A. Ren, J. Yang, X. Shen, X. Dong, Z. Zhao, and P. Dai, Phys. Rev. B **78**, 132504 (2008).
[21] Y. Qiu, W. Bao, Q. Huang, T. Yildirim, J. M. Simmons, M. A. Green, J. W. Lynn, Y. C. Gasparovic, J. Li, T. Wu, G. Wu, and X. H. Chen, Phys. Rev. Lett. **101**, 257002 (2008).
[22] S. A. J. Kimber, D. N. Argyriou, F. Yokaichiya, K. Habicht, S. Gerischer, T. Hansen, T. Chatterji, R. Klingeler, C. Hess, G. Behr, A. Kondrat, and B. Büchner, Phys. Rev. B **78**, 140503(R) (2008).
[23] H. Eschrig, arXiv:0804.0186 (unpublished).
[24] G. Xu, W. Ming, Y. Yao, X. Dai, S. C. Zhang, and Z. Fang, Europhys. Lett. **82**, 67002 (2008).
[25] K. Haule, J. H. Shim, and G. Kotliar, Phys. Rev. Lett. **100**, 226402 (2008).
[26] S. Ishibashi, K. Terakura, and H. Hosono, J. Phys. Soc. Jpn. **77**, 053709 (2008).
[27] T. Yildirim, Phys. Rev. Lett. **101**, 057010 (2008).
[28] J. Dong, H. J. Zhang, G. Xu, Z. Li, G. Li, W. Z. Hu, D. Wu, G. F. Chen, X. Dai, J. L. Luo, Z. Fang, and N. L. Wang, Europhys. Lett. **83**, 27006 (2008).
[29] F. Ma and Z. Y. Lu, Phys. Rev. B **78**, 033111 (2008).
[30] D. J. Singh and M.-H. Du, Phys. Rev. Lett. **100**, 237003 (2008).
[31] C. Cao, P. J. Hirschfeld, and H. P. Cheng, Phys. Rev. B **77**, 220506(R) (2008).
[32] Z.-Y. Weng, arXiv:0804.3228 (unpublished).
[33] F. Ma, Z. Y. Lu, and T. Xiang, Phys. Rev. B **78**, 224517 (2008).
[34] Z. P. Yin, S. Lebègue, M. J. Han, B. P. Neal, S. Y. Savrasov, and W. E. Pickett, Phys. Rev. Lett. **101**, 047001 (2008).
[35] Q. Si and E. Abrahams, Phys. Rev. Lett. **101**, 076401 (2008).
[36] C. Fang, H. Yao, W. F. Tsai, J. P. Hu, and S. A. Kivelson, Phys. Rev. B **77**, 224509 (2008).
[37] C. K. Xu, M. Müller, and S. Sachdev, Phys. Rev. B **78**, 020501(R) (2008).
[38] P. Blaha, K. Schwarz, G. K. H. Madsen, D. Kavasnicka, and J. Luitz, *WIEN2K: An Augmented Plane Wave+Local Orbitals Program for Calculating Crystal Properties* (Technische Universität, Wien, Austria, 2001).
[39] J. P. Perdew, K. Burke, and M. Ernzerhof, Phys. Rev. Lett. **77**, 3865 (1996).
[40] D. C. Koskenmaki and K. A. Gschneidner, Jr., *Handbook on the Physics and Chemistry of Rare Earths: Metal*, edited by K. A. Gschneidner, Jr. and L. Eyring (North Holland, Amsterdam, 1981), Vol. 1, Chap. 4.
[41] V. I. Anisimov, J. Zaanen, and O. K. Andersen, Phys. Rev. B **44**, 943 (1991).
[42] M. Cococcioni and S. de Gironcoli, Phys. Rev. B **71**, 035105 (2005).
[43] D. A. Andersson, S. I. Simak, B. Johansson, I. A. Abrikosov, and N. V. Skorodumova, Phys. Rev. B **75**, 035109 (2007).
[44] C. Loschen, J. Carrasco, K. M. Neyman, and F. Illas, Phys. Rev. B **75**, 035115 (2007).
[45] F. Tran, J. Schweifer, P. Blaha, K. Schwarz, and P. Novak, Phys. Rev. B **77**, 085123 (2008).
[46] I. A. Nekrasov, Z. V. Pchelkina, and M. V. Sadovskii, JETP Lett. **87**, 560 (2008).
[47] L. Pourovskii, V. Veronica, S. Biermann, and A. Georges, Europhys. Lett. **84**, 37006 (2008).